

METHODS

Injected Harmonic Feature Based Protection Scheme for Active Distribution Networks With High Proportion IIDGs

HAIYING YU¹, ZHONGFENG LU¹, YULIANG LIU¹, YANG GAO², AND JINGYING WAN³

¹Harbin Nengchuang Digital Technology Company Ltd., Harbin 150028, China

²School of Economics and Management, Harbin Normal University, Harbin 150500, China

³College of Electrical and Information Engineering, Hunan University, Changsha 410008, China

Corresponding author: Yuliang Liu (liuyuliang@harbin-electric.com)

ABSTRACT In distribution networks with a high proportion of inverter-interfaced distributed generators (IIDGs), the fault ride-through control strategy of the inverter affects the output current of IIDGs, causing limited amplitude and time-varying phase. This hinders the effectiveness of traditional protection schemes in safeguarding active distribution networks. To address this issue, a fault protection concept involving “active harmonic injection of IIDGs, harmonic layer establishment of the distribution network, and feature difference construction of internal and external faults” is proposed in this paper. Based on this concept, initially, the amplitude characteristics of actively injected harmonics are examined for both active lines equipped with IIDG interfaces and passive lines lacking interfaced IIDG. Following this analysis, protection criteria are established, taking into account the discrepancies between the two types of branches during fault occurrences. To boost system security and complete the protection strategy, the impedance at various frequencies is used for backup protection, making protection process more reliable. Especially, the designed main protection scheme exploits harmonic current differences between adjacent lines, enabling protection with minimal communication bandwidth, balancing efficiency and effectiveness. The proposed protection scheme is validated through MATLAB/Simulink simulations, considering various scenarios such as different fault resistances, fault locations, connection of nonlinear loads, failure of main protection and disconnection of some IIDGs. These simulation results demonstrate the effectiveness of the proposed protection scheme.


INDEX TERMS Harmonic injection, harmonic frequency-amplitude protection criteria, active distribution network, inverter interfaced distributed generators.

I. INTRODUCTION

As the proportion of distributed energy resources integrated into the power system continues to increase, the traditional distribution network is transitioning from a single-source radial power supply structure to a complex power supply structure with decentralized distribution from multiple sources. Active distribution networks, compared to traditional networks, exhibit the following characteristics: 1) Flexible and changeable network topology, with dynamic and bidirectional power flow in the distribution network; 2) Inverter-interfaced distributed generators (IIDGs) with

weak over-current capability and fast fault ride-through control response; 3) The amplitude and phase of fault currents outputted by IIDGs are limited and time-varying due to inverter control strategies and mode switching [1], [2], [3]. These characteristics, induced by a high proportion of IIDGs, pose challenges to the design of protection systems and can lead to maloperation of traditional over-current relays and differential protection. Consequently, protection has become a major challenge for active distribution networks with a high proportion of IIDGs.

To address this challenge, various methods have been studied to passively mitigate the impacts of IIDGs on active distribution networks, relying on the fault features of the system itself. Adaptive over-current protection, as mentioned

The associate editor coordinating the review of this manuscript and approving it for publication was Arturo Conde .

in [4] and [5], updates itself to protect networks but requires expensive communication and detailed system knowledge. The dual-setting directional over-current protection discussed in [6] sets different time-current characteristics for faults but doesn't adapt to network changes. Group-based over-current protection, from [1] and [7], clusters scenarios for optimal settings to reduce relay times. Distance protection, confirmed in [8], is essential but can be affected by IIDG output variability. References [9], [10], and [11] have looked into using high-frequency impedance for better distance protection. Differential protection, known for its selectivity from [12], [13], and [14], needs extensive communication and accurate data timing. Methods in [15], [16], [17], and [18] suggest using current and impedance variations for fault identification. Various protection strategies have been formulated and refined for active distribution networks to enhance reliability and fault management. Reference [19] introduces an adaptive protection strategy for active distribution networks with integrated DERs, enhancing fault detection and relay coordination without communication links by using local measurements to estimate network parameters across various operating modes. A new protection scheme for active distribution networks is proposed in [20], using power measurements to detect asymmetrical faults, ensuring quick and reliable backup protection. Orozco-Álvarez et al. presents a study on improving distance relay accuracy in active distribution networks with distributed energy resources, proposing a new strategy that compensates for fault resistance and current variations without needing communication [21].

Nevertheless, traditional protection schemes in active distribution networks take time to gather and analyze data before acting, and they rely on specific system details, making it hard to deal with unclear fault signs and complex network operations. IIDGs can quickly adjust and actively help during faults, providing new protection options. They act like extra sensors on the line, helping to spot and pinpoint faults. Even though one IIDG has a limited effect, many IIDGs working together can greatly improve fault detection and analysis, especially for upstream faults or when the network is isolated. As distributed generation tech improves and IIDGs become more common, they should shift from a passive role to a proactive one, using their control abilities to aid during faults.

While the active protection method of harmonic injection based on IIDG has not yet seen widespread application in active distribution networks, it has garnered considerable attention from researchers within the context of microgrids. To completely mitigate the adverse influence of conventional control and fault ride-through control strategies of IIDGs on protection design, injected harmonic-based methods have been proposed to actively construct harmonic fault features that are independent of the fundamental fault features of the distribution network [22], [23], [24], [25]. The measured impedance and injected harmonic current are used as fault indicators. Moreover, the harmonic current versus fault impedance droop control of IIDGs, combined with the

inverse-time principle, is adopted to achieve selective coordination of protection devices. However, the over-current relays in [22] and [23] may have difficulty adapting to the flexible topology of the system. The coordination time of harmonic directional over-current relays based on the inverse-time principle may result in a prolonged fault clearing time for high impedance faults [24], [25]. Reference [24] introduced a specific percentage of the fifth harmonic into the fault current, utilizing the distinctive properties of the harmonic current to differentiate between the fault current and variations in load current.

From the perspective of communication requirements, the above-mentioned research can be categorized into double-ended protection and single-ended protection systems. Single-ended protection systems are cost-effective and structurally straightforward, but they are limited in terms of accuracy and selectivity. This type of protection method may be suitable for shorter distances or lines that are not critical to the overall system. On the other hand, dual-ended protection systems, while more expensive and complex, provide higher accuracy and selectivity in fault detection, which is why they are usually preferred for long-distance or critical lines within the system.

Therefore, employing dual-ended protection as the primary protection method and single-ended protection as the backup is considered a high-quality solution. This approach ensures that the most critical parts of the system are guarded by the most reliable protection while still providing a cost-effective and simpler protection method for less critical areas.

In this paper, the harmonic feature difference between external and internal faults of active distribution network with a high proportion of IIDGs is analyzed, utilizing the flexible controllability of IIDGs. Based on this analysis, a scheme is proposed that includes harmonic injection and the design of protection criteria. This scheme comprises both main protection and backup protection mechanisms based on current and impedance characteristics, respectively. In this scheme, fixed harmonics are generated during faults by controlling IIDGs to inject the required harmonics. Additionally, a harmonic frequency-amplitude cooperative protection criteria is constructed. This scheme inherently performs fault phase selection by capitalizing on the distinct characteristics of harmonic currents produced by various fault types. It is worth noting that the proposed scheme of main protection only requires current measurement and low bandwidth communication, while the protection performance of both main and backup protection is not affected by fault conditions, the permeability, the connection of nonlinear loads, and disconnection of IIDGs. The comprehensive comparison of the different protection methods discussed in this paper is presented in Table 1. The method proposed enhances protection in active distribution networks by balancing communication efficiency, fault resistance sensitivity, and a broad acceptance angle, while also incorporating backup protection and phase selection capabilities for precise fault localization.

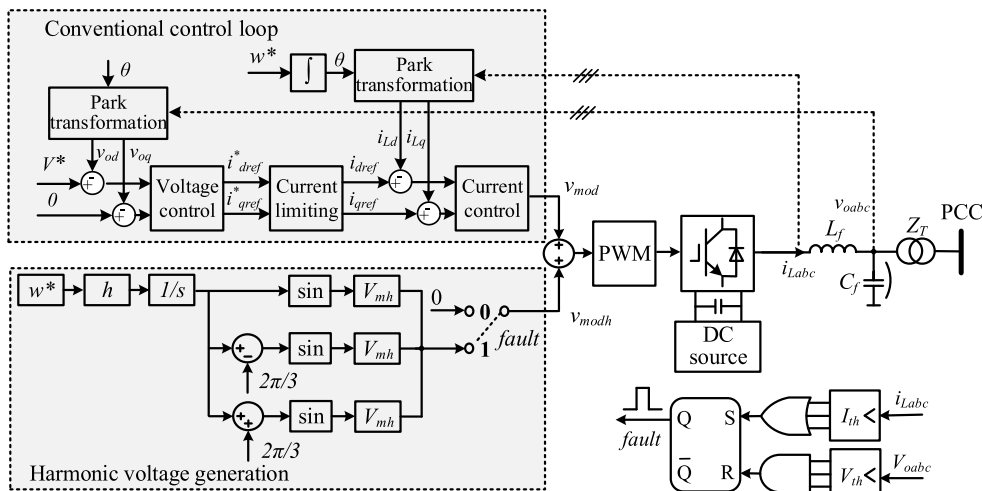


FIGURE 2. Harmonic injection control structure.

can adopt neutral ungrounding, neutral resonant grounding, or neutral high-resistance grounding modes. In the event of a single-phase ground fault in a small current grounding system, the fault phase voltage decreases, while the non-fault phase voltage can rise up to $\sqrt{3}$ times the rated value. However, the phase-to-phase voltage remains relatively unchanged. As a result, the single-phase to ground fault current is very weak, and the distribution network can continue to supply power for a certain period of time. Therefore, in this paper, the protection of distribution networks with high proportions of IIDGs against three-phase short-circuit faults, phase-to-phase faults, and two-phase to ground faults is primarily focused on.

A. HARMONIC LAYER ESTABLISHMENT OF ACTIVE DISTRIBUTION NETWORK

In order to preserve the stability and power quality of the distribution network, the injection of harmonics is not continuous but triggered only after a disturbance is detected. Each IIDG in the network independently determines whether to inject harmonics. When a fault is detected, harmonic injection is triggered without the need for additional per-processing steps. To establish the difference in harmonic characteristics between internal and external fault currents, all IIDGs in the distribution network inject harmonic currents of different frequencies.

The harmonic current injection control of IIDGs is shown in Figure 2. Among this, the voltage control loop and current control loop are implemented to ensure stable regulation of voltage and current [26], [27]. A fixed amplitude and frequency harmonic voltage is added to the modulation voltage outputted by the conventional control loop.

It is important to ensure that all harmonic frequencies are lower than the cutoff frequency of the output filter of the IIDG inverter to prevent the injected harmonic current from being filtered out. As the injected harmonic current is proportional

to the harmonic voltage generated by IIDGs, the amplitude V_{mh} of the harmonic voltage must satisfy Equation (1) to prevent the IIDG output fault current from exceeding its maximum allowable value I_{th} . Here, I_{lim} represents the limited value of the fundamental current amplitude.

$$V_{mh} \leq (I_{th} - I_{lim})Z_{DG} \tag{1}$$

Furthermore, the activation of harmonic injection control is determined by the fault detection module, which follows the current-set and voltage-reset strategy depicted in Figure 2. When the instantaneous current i_{Labc} outputted by IIDGs exceeds its maximum allowable value $I_{th} = 2$ p.u. in at least one phase, the “fault” signal is set to 1. After the fault is cleared, the inverter returns to normal operation when the amplitudes V_{oabc} of the three-phase output voltage are all greater than the threshold V_{th} .

B. HARMONIC CURRENT FEATURE DIFFERENCE BETWEEN INTERNAL AND EXTERNAL FAULTS

1) HARMONIC CURRENT CHARACTERISTICS OF ACTIVE BRANCHES

In this paper, the analysis considers five IIDGs denoted as $IIDG_i$, ($i = 1, 2, \dots, 5$) and fault resistances R_{Fj} , ($j = 1, 2, \dots, 6$) corresponding to faults F_1 to F_6 as shown in Figure 1. Accordingly, the orders of injected harmonics are h_i , ($i = 1, 2, \dots, 5$). Z_{Lk} is the load impedance of $Load_k$, ($k = 1, 2, 3, 4$). \dot{V}_{DG}^{hi} and Z_{DG}^{hi} are the h_i -th harmonic voltage source and output impedance of $IIDG_i$. The fault analysis is conducted using the superposition theorem, where only $IIDG_i$ injects harmonics into the distribution network while the other IIDGs are treated as short circuits.

a: THE LINE ON WHICH ONLY ONE SIDE IS CONNECTED WITH IIDG

Thus, under a three-phase to ground fault at F_1 , the simplified fault phase equivalent circuits of distribution network at

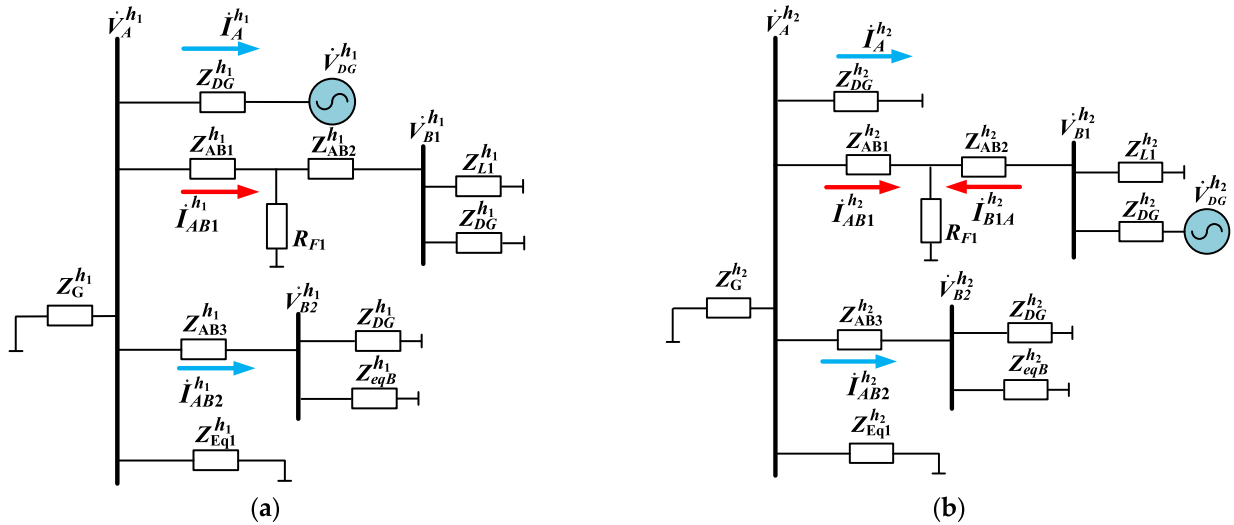


FIGURE 3. After a fault occurs at F_1 , the simplified equivalent circuit of distribution network at different harmonic layers. (a) at h_1 -th harmonic layer; (b) at h_2 -th harmonic layer.

h_1 -th, h_2 -th and h_3 -th harmonics are shown in Figure 3(a), (b) and (c), respectively.

The direction of the outflow bus is the reference positive direction. $\dot{V}_A^{h_i}$, $\dot{V}_{B1}^{h_i}$, and $\dot{V}_{B2}^{h_i}$ are the h_i -th harmonic voltages at BusA, BusB1, and BusB2, respectively. $i_{AB1}^{h_i}$, $i_{AB2}^{h_i}$, and $i_A^{h_i}$ are the h_i -th harmonic currents flowing from BusA. $Z_{AB1}^{h_i}$, $Z_{AB2}^{h_i}$, $Z_{AB3}^{h_i}$, and $Z_{BC}^{h_i}$ are the equivalent line impedances under the h_i -th harmonic. $Z_{Eq1}^{h_i}$ is the corresponding equivalent impedance of other passive branches. Likely, $Z_{eqB}^{h_i}$ is the equivalent impedance at BusB2.

According to Figure 3 (a), the fault line current when only IIDG₁ is considered is,

$$i_{AB1}^{h_1} = \frac{\dot{V}_{DG1}^{h_1} \left[Z_{M1}^{h_1} // Z_{Eq1}^{h_1} // Z_G^{h_1} // \left(Z_{AB3}^{h_1} + Z_{DG}^{h_1} // Z_{eqB}^{h_1} \right) \right]}{Z_{M1}^{h_1} \left[Z_{M1}^{h_1} // Z_{Eq1}^{h_1} // Z_G^{h_1} // \left(Z_{AB3}^{h_1} + Z_{DG}^{h_1} // Z_{eqB}^{h_1} \right) + Z_{DG}^{h_1} \right]} \quad (2)$$

where, $Z_{M1}^{h_1} = \left(Z_{AB2}^{h_1} + Z_{L1}^{h_1} // Z_{DG}^{h_1} \right) // R_{F1} + Z_{AB1}^{h_1}$

The harmonic current $i_A^{h_1}$ is flowing from IIDG₁ into BusA, which has opposite direction.

$$i_A^{h_1} = - \frac{\dot{V}_{DG1}^{h_1}}{Z_{M1}^{h_1} // Z_{Eq1}^{h_1} // Z_G^{h_1} // \left(Z_{AB3}^{h_1} + Z_{DG}^{h_1} // Z_{eqB}^{h_1} \right) + Z_{DG}^{h_1}} \quad (3)$$

The harmonic current $i_{AB2}^{h_1}$ can be described as (4), shown at the bottom of the page.

In Equations (1)-(4), when $R_{F1} = 0$, $|i_A^{h_1}| > |i_{AB1}^{h_1}| > |i_{AB2}^{h_1}|$ is satisfied. The maximum value of h_1 -th harmonics appears only in the branch connected to IIDG₁ and the harmonic current direction is negative, which is also effective for the fault scenario of $R_{F1} \neq 0$.

For the phase-to-phase faults and two phase to ground faults, the harmonic currents can be obtained by substituting $i_{AB1}^{h_1} = i_{AB1\phi1}^{h_1} - i_{AB1\phi2}^{h_1}$ into (4), whose expressions are the same as that of three-phase faults. The subscripts ϕ_1 and ϕ_2 represent two fault phases. Therefore, the analysis focuses on the harmonic current characteristics of active distribution networks using a three-phase to ground fault as an example.

According to Figure 3(b), when only IIDG₂ is considered, the harmonic current $i_{AB1}^{h_2}$ of fault line is described as shown in Equation (5), which has the positive direction.

$$i_{AB1}^{h_2} = \frac{-\dot{V}_{DG}^{h_2} R_{F1} \left(Z_{M2}^{h_2} - Z_{DG}^{h_2} \right)}{Z_{M3}^{h_2} \left[\left(Z_{M2}^{h_2} // R_{F1} \right) + Z_{AB2}^{h_2} \right] \left[R_{F1} // \left(Z_{M2}^{h_2} + Z_{AB1}^{h_2} \right) \right]} \quad (5)$$

where, $Z_{M2}^{h_2} = Z_{Eq1}^{h_2} // Z_G^{h_2} // Z_{DG}^{h_2} \left(Z_{AB3}^{h_2} + Z_{DG}^{h_2} // Z_{eqB}^{h_2} \right)$, $Z_{M3}^{h_2} = Z_{M2}^{h_2} // Z_{M1}^{h_2}$.

The harmonic currents $i_A^{h_2}$ and $i_{AB2}^{h_2}$ are described as Equations (6) and (7), as shown at the bottom of the next page, respectively.

$$i_{AB2}^{h_1} = \frac{\dot{V}_{DG1}^{h_1} \left[Z_{M1}^{h_1} // Z_{Eq1}^{h_1} // Z_G^{h_1} // \left(Z_{AB3}^{h_1} + Z_{DG}^{h_1} // Z_{eqB}^{h_1} \right) \right]}{\left(Z_{AB3}^{h_1} + Z_{DG}^{h_1} // Z_{eqB}^{h_1} \right) \left[Z_{M1}^{h_1} // Z_{Eq1}^{h_1} // Z_G^{h_1} // \left(Z_{AB3}^{h_1} + Z_{DG}^{h_1} // Z_{eqB}^{h_1} \right) + Z_{DG}^{h_1} \right]} \quad (4)$$

From (5)-(7), when $R_{F1} = 0$, $i_A^{h2} = i_{AB1}^{h2} = i_{AB2}^{h2} = 0$ is satisfied, i.e., the harmonic currents cannot pass through the fault point. When $R_{F1} \neq 0$, the amplitude relationship of i_A^{h2} , i_{AB1}^{h2} and i_{AB2}^{h2} are positively correlated to the fault resistance.

Moreover, since the fault resistance is usually much smaller than the load impedance and the equivalent impedance of IIDG, the amplitude of i_{AB1}^{h2} is much smaller than that of i_{B1A}^{h2} , i.e., $|i_{AB1}^{h2}| \ll |i_{B1A}^{h2}|$ is satisfied. The harmonic current on one side of the fault line connected to IIDG will be much greater than that of the other side.

According to Figure 4, when only IIDG₃ is considered, the harmonic current of fault line is i_{AB1}^{h1} ,

$$i_{AB1}^{h3} = \frac{\dot{V}_{DG}^{h3} (Z_{M3}^{h3} - Z_{DG}^{h3}) (Z_G^{h3} // Z_{Eq1}^{h3} // Z_{DG}^{h3} // Z_{M1}^{h3})}{Z_{AB3}^{h3} Z_{M3}^{h3} Z_{M1}^{h3}} \quad (8)$$

The harmonic currents i_A^{h3} and i_{AB2}^{h3} can be described as,

$$i_A^{h3} = \frac{\dot{V}_{DG}^{h3} (Z_{M3}^{h3} - Z_{DG}^{h3}) (Z_G^{h3} // Z_{Eq1}^{h3} // Z_{DG}^{h3} // Z_{M1}^{h3})}{Z_{AB3}^{h3} Z_{M3}^{h3} Z_{DG}^{h3}} \quad (9)$$

$$i_{AB2}^{h3} = -\frac{\dot{V}_{DG}^{h3} (Z_{M3}^{h3} - Z_{DG}^{h3})}{Z_{AB3}^{h3} Z_{M3}^{h3}} \quad (10)$$

Similarly, according to (8)-(10), $|i_{AB2}^{h3}| > |i_{AB1}^{h3}| > |i_A^{h3}|$ is satisfied. The maximum value of h_3 -th harmonics appears only in the branch connected to IIDG₃ and the harmonic current direction is negative.

In Figure 5, the blue arrow represents the harmonic current distribution injected by IIDG₁ to IIDG₃. For the fault line AB1, the harmonic currents at the head-end of fault line have positive directions, i.e., the fault direction is forward. The harmonic currents at the remote-end of fault line have negative directions, i.e., the fault direction is backward. For the non-fault section AB2, the harmonic currents measured by the IED at the head and end of fault line have negative directions.

b: THE LINE ON WHICH BOTH SIDES ARE CONNECTED WITH IIDGS

Figure 6 illustrates the distribution of h_3 -th and h_4 -th harmonic currents when a fault occurs at F₂. The equivalent impedance of the other passive branches is represented by Z_{Eq}^{h34} . The blue arrows indicate the direction of the harmonic currents. Based on the direction of the harmonic currents

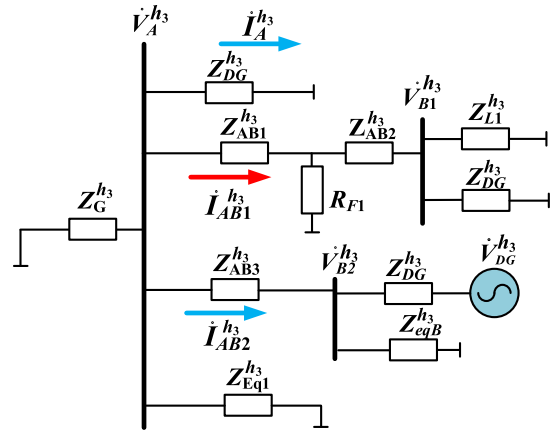


FIGURE 4. After a fault occurs at F₁, the simplified equivalent circuit of distribution network at h_3 -th harmonic layer.

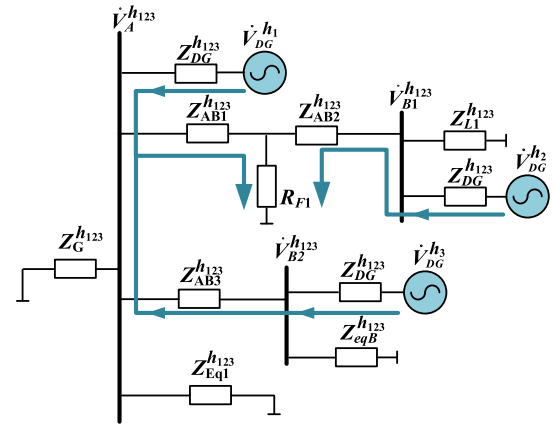


FIGURE 5. After a fault occurs at F₁, the simplified equivalent circuit of distribution network at h_1 -th to h_3 -th harmonics layer.

shown by the blue arrows, it can be observed that the harmonic current characteristics of the active branches, where both sides are connected with IIDGs, are the same as the active branch where only one side is connected with IIDG.

Specially, according to Figures 6 and 7, F₃ and F₂ are two fault points in the upstream and downstream section on the same branch. When a fault occurs at F₃, for the fault Line C1D, the harmonic currents at the head-end of fault line have positive directions, i.e., the fault direction is forward. The harmonic currents at the remote-end of fault line have negative directions, i.e., the fault direction is backward. For the

$$i_A^{h2} = \frac{\dot{V}_{DG}^{h2} R_{F1} Z_{M2}^{h2} (Z_{M2}^{h2} - Z_{DG}^{h2})}{Z_{M3}^{h2} Z_{DG}^{h2} \left[\left(\frac{Z_{M2}^{h2}}{R_{F1}} \right) + Z_{AB2}^{h2} \right] \left[R_{F1} // \left(Z_{M2}^{h2} + Z_{AB1}^{h2} \right) \right]} \quad (6)$$

$$i_{AB2}^{h2} = \frac{\dot{V}_{DG}^{h2} R_{F1} Z_{M2}^{h2} (Z_{M2}^{h2} - Z_{DG}^{h2})}{Z_{M3}^{h2} \left(Z_{AB3}^{h2} + Z_{DG}^{h2} // Z_{eqB}^{h2} \right) \left[\left(\frac{Z_{M2}^{h2}}{R_{F1}} \right) + Z_{AB2}^{h2} \right] \left[R_{F1} // \left(Z_{M2}^{h2} + Z_{AB1}^{h2} \right) \right]} \quad (7)$$

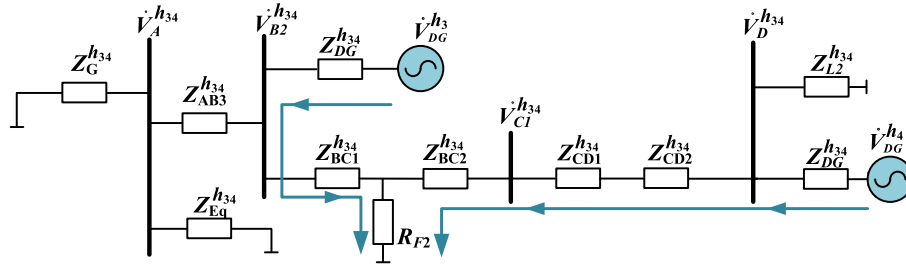


FIGURE 6. After a fault occurs at F_2 , the simplified equivalent circuit of distribution network at h_3 -th and h_4 -th harmonic layers.

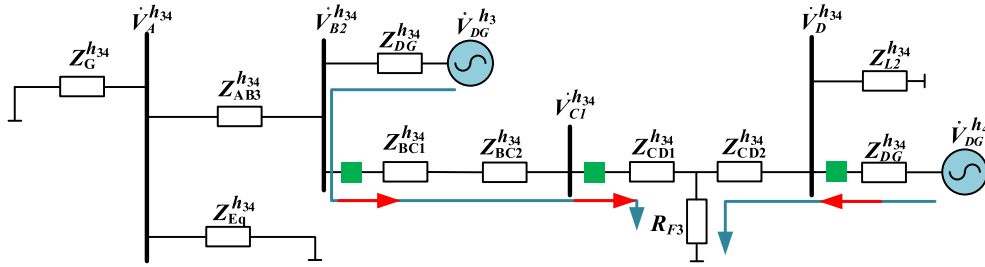


FIGURE 7. The harmonic current direction and fault direction when a fault occurs on the downstream section of the active branch on which both sides are connected with IIDGs.

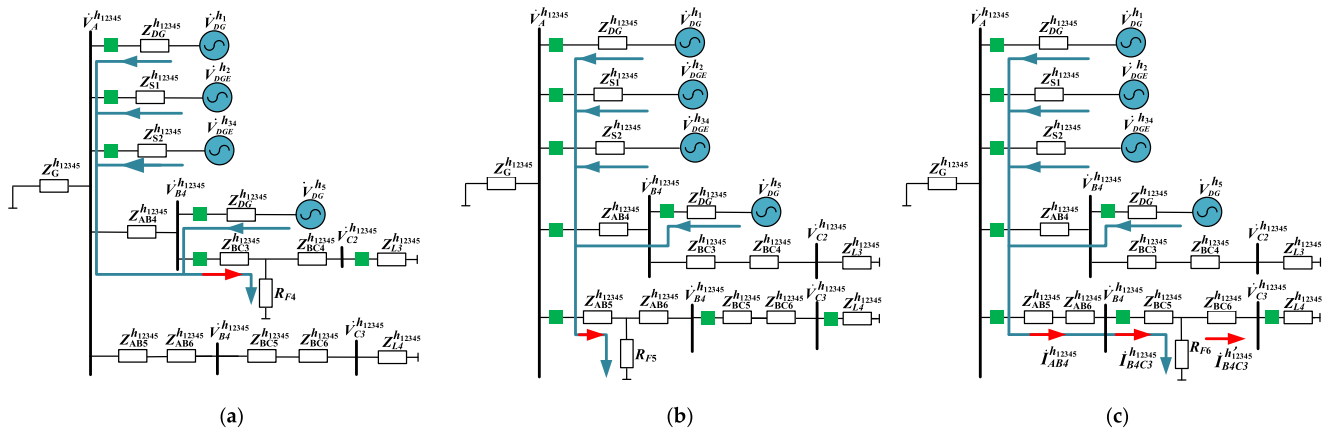


FIGURE 8. After a fault occurs at F_4 - F_6 , the simplified equivalent circuit of distribution network at harmonic layers. (a) A fault occurs at F_4 ; (b) A fault occurs at F_5 ; (c) A fault occurs at F_6 .

upstream non-fault *Line*B2C1, the harmonic currents at the head and remote-ends of fault line have positive directions.

2) HARMONIC CURRENT CHARACTERISTICS OF PASSIVE BRANCHES

Figure 8 (a)-(c) depicts the distribution of harmonic currents when a fault occurs at F_4 - F_6 . To simplify the circuit and enhance the clarity of harmonic direction, all impedances in the branch where IIDG₂, IIDG₃, and IIDG₄ are located are equivalently represented by Z_{S1} and Z_{S2} , respectively. It is evident that the fault direction, as measured by the IEDs on both sides of the non-fault line, is backward. However, the fault directions, as measured by the IEDs on both sides of the fault line, are forward and backward, respectively.

In cases where the passive branch consists of upstream and downstream sections, the fault direction measured by the IED at the head of the fault line aligns with that measured by the IED at the head of the upstream non-fault line.

In Figure 8(c), $i_{B4C3}^{h_{12345}}$ is the harmonic currents flowing into fault point F_4 . $i_{B4C3}^{h_{12345}}$ is the harmonic currents flowing from fault point into BusC2. The relationship between $i_{B4C3}^{h_{12345}}$ and $i_{B4C3}^{h_{12345}}$ is described as,

$$i_{B4C3}^{h_{12345}} = i_{B4C3}^{h_{12345}} \frac{R_{F6}}{R_{F6} // (Z_{BC6}^{h_{12345}} + Z_{L4}^{h_{12345}})} \quad (11)$$

When $R_{F6} = 0$, $i_{B4C3}^{h_{12345}} = 0$ is satisfied, i.e., the harmonic current cannot pass through the fault point. For case where

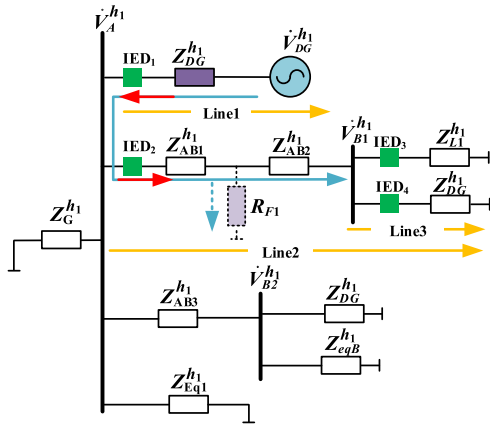


FIGURE 9. Network impedance variation due to injection of h_1 -th harmonic before and after fault occurs at F_1 .

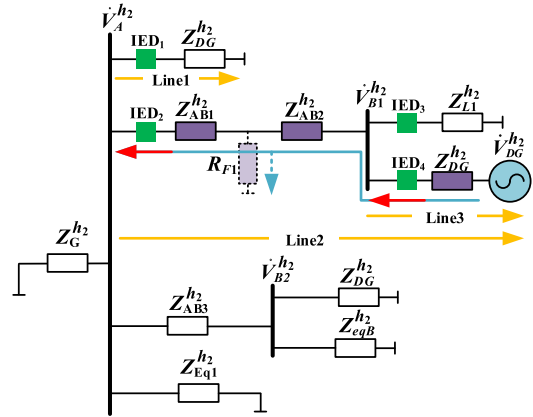


FIGURE 10. Network impedance variation due to injection of h_2 -th harmonic before and after fault occurs at F_1 .

$R_{F6} \neq 0$, since the load impedance Z_{L4} is usually much larger than line impedance Z_{BC6} and fault resistance R_{F6} , the amplitude of i_{B4C3}^{h1} is usually much smaller than that of i_{B4C3}^{h2} , and $|i_{B4C3}^{h1}| \ll |i_{B4C3}^{h2}|$ are satisfied. That is, the harmonic current on one side of fault line will be much greater than that of the other side.

C. IMPEDANCE FEATURE DIFFERENCE BETWEEN INTERNAL AND EXTERNAL FAULTS

Figure 9 depicts the variations in network impedance before and after the fault F_1 , influenced by the h_1 -th harmonic injected by IIDG₁. Similarly, the changes in system impedance before and after the occurrence of fault F_1 , with the application of IIDG₂, are shown in Figure 10. Following the fault, the impedance of Line 2 is equivalent to a parallel connection with the fault resistor R_{F1} , while the impedance of Line 1 remains the same. Z_{Line1}^{hi} ($i = 1, 2$) represents the impedance of Line 1 before the fault, and $Z_{Line1}^{h'i}$ represents the impedance of Line1 after the fault has occurred, with both impedance values being Z_{DG}^{hi} , as indicated in Equations 12. Note that Z_*^{hi} is the impedance of Line * before the fault, then $Z_*^{h'i}$ represents the impedance after the fault has occurred, the equivalent impedances of Line 2, Line AB1, and Line 3 before and after the fault occurrence are presented in Equations (12)-(14).

$$Z_{Line1}^{hi} = Z_{DG}^{hi}, Z_{Line1}^{h'i} = Z_{DG}^{hi} \quad (12)$$

$$Z_{Line2}^{hi} = Z_{AB1}^{hi} + Z_{AB2}^{hi} + Z_{L1}^{hi} // Z_{DG}^{hi}$$

$$Z_{LineAB1}^{hi} = Z_{AB1}^{hi} + Z_{AB2}^{hi}$$

$$Z_{Line3}^{hi} = Z_{DG}^{hi} \quad (13)$$

$$Z_{Line2}^{h'i} = Z_{AB1}^{h'i} + R_{F1} // (Z_{AB2}^{h'i} + Z_{L1}^{h'i} // Z_{DG}^{h'i})$$

$$Z_{LineAB1}^{h'i} = Z_{AB1}^{h'i} + R_{F1} // Z_{AB2}^{h'i}$$

$$Z_{Line3}^{h'i} = Z_{DG}^{h'i} \quad (14)$$

It is known that the fault resistance is typically much lower than both the load impedance and the equivalent impedance of the IIDG. Therefore, it can be inferred that a considerable change in the equivalent impedance will occur on Line 2 where the fault happened, and the equivalent impedance of Line AB1 will also experience a notable shift. However, the equivalent impedance of Line 3, despite being in the vicinity of Line 2, will remain unchanged. Therefore, it can be inferred that within an active branch containing both passive and active lines with an upstream and downstream relationship, a fault occurring on a particular line level will not impact the impedance of the lines upstream and downstream of it.

In addition to the expressions shown in Equations (12)-(14), the impedance of the line can also be expressed as

$$Z = R + \omega(L + C) \quad (15)$$

It is clear that the magnitude of the imaginary part of the impedance in the line is closely related to the frequency that is injected. In Figures 9 and 10, the impedances produced by IIDG₁ and IIDG₂ can be analyzed for IED1 at the head-end of Line 1, with the effective value of their imaginary parts expressed as $|\text{Im}(Z_{Line1}^{hi})|$ ($i = 1, 2$). Similarly, analyses for IED2 and IED4 yield values $|\text{Im}(Z_{LineAB1}^{hi})|$ and $|\text{Im}(Z_{Line3}^{hi})|$, respectively. According to Equations (12)-(14), it can be observed that after a fault occurs, $|\text{Im}(Z_{Line1}^{h'i})|$ will not change, while $|\text{Im}(Z_{LineAB1}^{h'i})| < |\text{Im}(Z_{LineAB1}^{hi})|$. The impedance generated by IIDG₂, corresponding to the branch where Line AB1 is located, approaches zero. For Line 3, the value of $|\text{Im}(Z_{Line3}^{h'i})|$ approaches zero while $|\text{Im}(Z_{Line3}^{h'i})|$ remains unchanged.

Figure 11 illustrates the variations in impedance of an active branch with established upstream and downstream relationships when a fault transpires. Mirroring the methodology of the preceding analysis, it can be deduced that subsequent to the fault occurrence, the value of $|\text{Im}(Z_{Line1B2C1}^{h'3})|$ remains unaffected, and the impedance

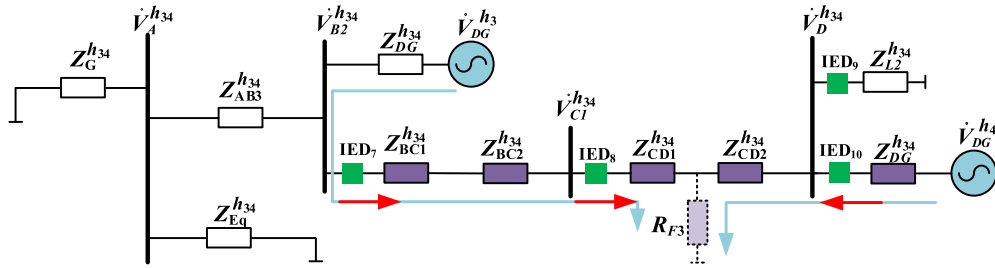


FIGURE 11. Network impedance variation due to injection of h_3 -th and h_4 -th harmonics before and after fault occurs at F_3 .

TABLE 2. The injected harmonic current characteristics on the active and passive branches (lines).

Branch status	Internal fault	External fault
Active	At the head-end of the line, the amplitude of harmonic current (hi) injected by the IIDG i connected to this branch(line) is detected to be minimum; Fault direction is forward At the remote-end of the line, the amplitude of harmonic current (hi) injected by the IIDG i connected to this branch(line) is detected to be maximum; Fault direction is backward	At the head-end of the line, the amplitude of harmonic current (hi) injected by the IIDG i connected to this branch(line) is detected to be maximum; Fault direction is backward
Passive	The amplitudes of the harmonic currents at the head-end are much larger compared to those at the remote-end.	The harmonic current amplitudes at the head-end are equal to those at the remote-end.

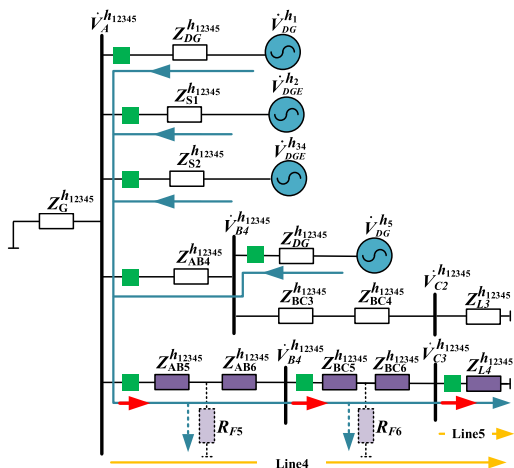


FIGURE 12. Network impedance variation due to injection of harmonics before and after a fault occurs at F_5 and F_6 .

denoted as $|\text{Im}(Z_{LineB2C1}^{h_4})|$, which is generated by IIDG4 in association with the branch where Line B2C1 is situated, tends towards zero.

Figure 12 demonstrates the impedance variation in a passive branch during a fault. It is evident that the impedance generated by the upstream line remains unchanged before and after the fault, regardless of the influence of different harmonics. However, the impedance of the downstream line approaches zero after the fault. Additionally, the impedance at the fault location experiences a significant decrease when affected by various harmonics after the fault.

D. SUMMARY OF HARMONIC CHARACTERISTICS

Overall, for the active distribution networks with high proportion IIDGs, the injected harmonic current characteristics on the active and passive branches (lines) can be summarized in Table 2.

In this paper, it is assumed that specific harmonics are injected by each IIDG before the network becomes operational, and the initial impedance values of the corresponding branches (lines) are recorded by IED at the head-end of each line. Correspondingly, the harmonic characteristics observed on both the passive and active branches (lines) during harmonic injection are summarized in Table 3.

III. PROPOSED PROTECTION SCHEME

A. PROTECTION CRITERIA

According to the analysis in Section II-B, the following protection criteria of main protection can be concluded. For active branches, the fault features of internal faults are characterized by opposite fault directions detected by two adjacent IEDs. Specifically, the IED at the head-end of the line detects a positive fault direction, while the IED at the end of the line detects a negative fault direction. On the other hand, the fault features of external faults are identified by a negative fault direction detected by the IED at the head-end of the line. For passive branches, the fault feature of internal faults is indicated by significantly smaller amplitudes of all harmonic currents detected by the IED at the remote-end compared to those detected by the IED at the head-end of the line. Conversely, the fault features of external faults are characterized by equal harmonic current amplitudes at both the head-end and the remote-end of the line.

TABLE 3. The impedance characteristics on the active and passive branches(lines) when injecting harmonics.

Branch status	Internal fault	External fault
Active	The effective value of the imaginary part of the impedance generated by the IIDG located on this line approaches zero	The effective value of the imaginary part of the impedance generated by the IIDG located on this line approaches zero The effective values of the imaginary part of the impedance generated by other IIDGs on this line remain unchanged
	The effective values of the imaginary part of the impedance generated by other IIDGs on this line significantly decrease	The effective value of the imaginary part of the impedance generated by the IIDG located on this line remains unchanged The effective values of the imaginary part of the impedance generated by other IIDGs on this line approach zero
Passive	The effective values of the imaginary part of the impedance generated by all IIDGs on this line are significantly reduced	The effective values of the imaginary part of the impedance generated by all IIDGs on this line tend to approach zero or The effective values of the imaginary part of the impedance generated by all IIDGs on this line remain unchanged

Based on these fault features, the frequency and corresponding amplitude of all harmonic currents injected by IIDGs can be utilized to establish main protection criteria for active and passive branch line identification as shown in Equations (15) and (16), respectively. Among them, $\dot{i}_{h_i}^{hm}$ is the current measurement value of the line head-end, $\dot{i}_{h_i}^{rm}$ represents the current measurement value of the line remote-end, and N is the number of IIDGs connected to the active distribution network.

Internal fault of active branch(line) for main protection:

$$\begin{cases} |\dot{i}_{h_n}^{hm}| > |\dot{i}_{h_i}^{hm}|, (i \neq n, i = 1, 2, \dots, N; n = 1, 2, \dots, N) \\ |\dot{i}_{h_n}^{rm}| < |\dot{i}_{h_i}^{rm}|, (i \neq n, i=1, 2, \dots, N; n = 1, 2, \dots, N) \end{cases} \quad (16)$$

Internal fault of passive branch(line) for main protection:

$$|\dot{i}_{h_i}^{hm}| \gg |\dot{i}_{h_n}^{rm}|, (i = 1, 2, \dots, N) \quad (17)$$

Analyzing the current and impedance characteristics at the time of fault occurrence allows for the establishment of a protection criterion for backup protection. This backup protection is a single-ended approach that operates independently of communication, providing a safeguard in the event that the main protection fails.

For active branches with internal faults, the imaginary part of the impedance generated from the IIDG on this line approaches zero, while the ones from other IIDGs significantly decreases. In the case of external faults on active branches, there are two sufficient conditions to distinguish. One is the imaginary part of the impedance generated from the IIDG on this line approaches zero, while the ones from other IIDGs remain unchanged. The second condition is that the imaginary part of the impedance generated from the IED on this line remains constant, while the imaginary parts generated from the other IIDGs approach zero. For passive branches, internal faults are marked by notable shifts in all impedance values. Similar to active branch, there are two scenarios indicating external faults: either the effective values of the imaginary part of the impedance produced by all IIDGs on this line tend to approach zero, or they remain unchanged

Utilizing these fault characteristics, the frequencies and corresponding amplitudes of all harmonic currents injected by IIDGs can be leveraged to formulate backup protection criteria. These criteria are used for identifying faults in active and passive branches(lines), and are outlined in Equations (18) and (19), respectively. Among them, $|\text{Im}(Z_{Line*}^{h_i})|$ is the effective value of the imaginary part of the impedance generated by the IIDG_{*i*} on Line*before fault occurs, $|\text{Im}(Z_{Line*}^{h'_i})|$ represents the one after fault.

Internal fault of active branch(line) for backup protection:

$$\begin{cases} |\text{Im}(Z_{Line*}^{h_i})| \approx 0, (i = 1, 2, \dots, N) \\ |\text{Im}(Z_{Line*}^{h_n})| > |\text{Im}(Z_{Line*}^{h'_n})|, (n \neq i, n = 1, 2, \dots, N) \end{cases} \quad (18)$$

Internal fault of passive branch(line) for backup protection:

$$|\text{Im}(Z_{Line*}^{h_i})| > |\text{Im}(Z_{Line*}^{h'_i})|, (i = 1, 2, \dots, N) \quad (19)$$

B. PROTECTION FLOWCHART

The flowchart of the injected harmonic feature based protection scheme for the active distribution networks with high proportion IIDGs is shown in Figure 13. The hardware requirements for the implementation of proposed protection scheme include: 1) The IED installed at each line records that whether the protected branch is a active branch, and collect the three-phase current from all CTs (current transformers) installed at head of the line, as well as collecting voltage from all PTs (potential transformers); 2) The communication channels are available between adjacent IEDs; 3) $|Z_{Line*}^{h_i}|$ are recorded before the network is operational.

Once the protection program is activated, the system initiates a timing sequence. First, the currents at head of all the lines are measured, and the amplitudes of all harmonic currents $\dot{i}_{h_i}^{rm}$ injected by IIDGs are extracted. During the timing phase of the protection process, the IED on the current line is responsible for transmitting current information to the IED on the up-stream line. Simultaneously, it awaits the receipt of information from the IED on the down-stream line.

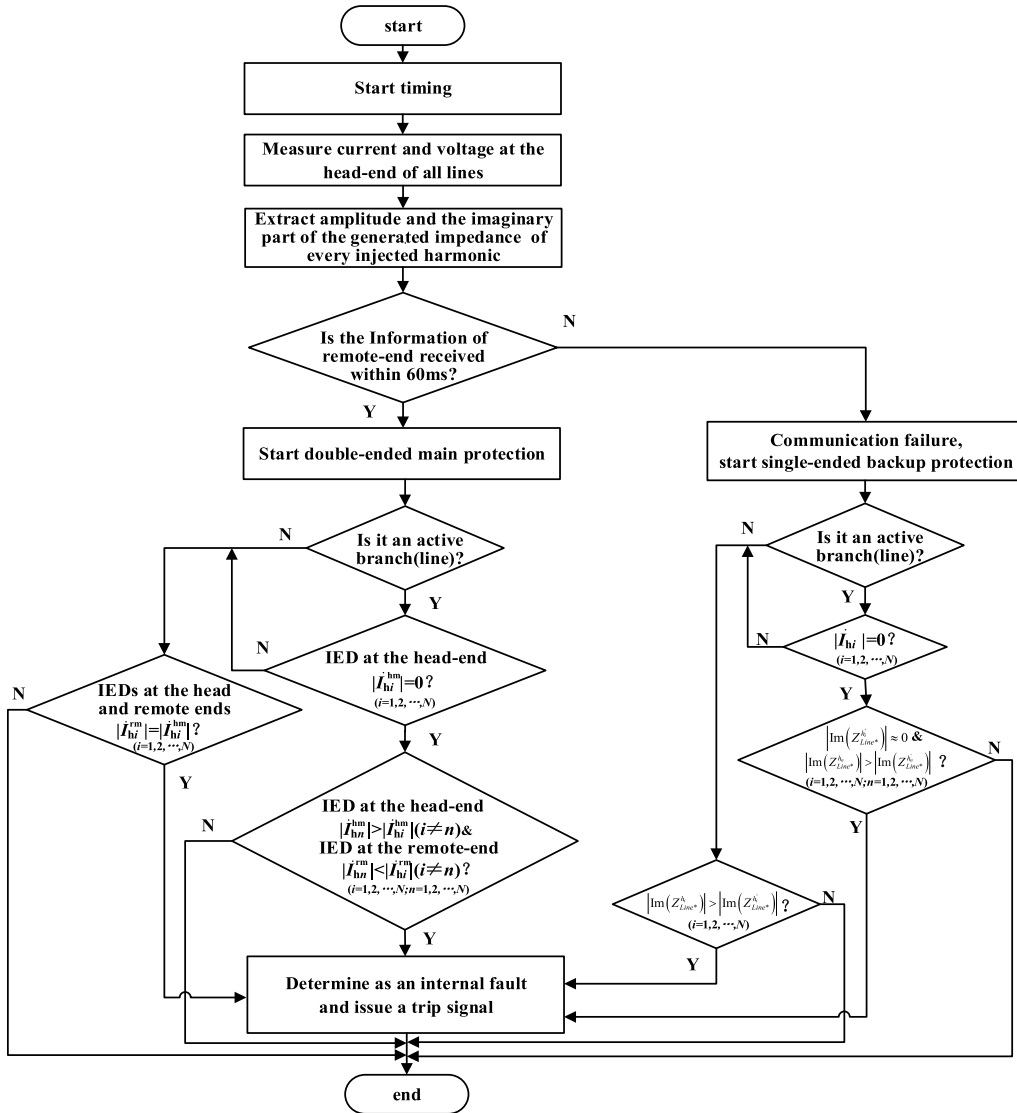


FIGURE 13. Protection flowchart.

Considering that an IIDG can output a fault current up to twice its rated value within a quarter cycle of the fundamental frequency [28], the required fault detection time to activate IIDG harmonic injection control is under 5ms. Moreover, the intrinsic response time for a circuit breaker is approximately 30ms [23]. FFT analysis reveals that it takes around 20ms to calculate the current amplitude at each frequency. The communication delay between adjacent IEDs is about 2ms. Consequently, the delay ΔT that assists the main protection criterion is set to 60 milliseconds.

If this exchange of information takes longer than ΔT , the delay is interpreted as a communication fault. In response to such a fault, the system is designed to activate backup protection measures to ensure continued system protection and reliability despite the communication issue.

In main protection, for the active branch(line), when the minimum amplitude of the harmonic current measured by

the IED at head of the protected line is injected by the connected IIDG_i, and the the maximum amplitude of the harmonic current measured by the IED at remote-end of the protected line is injected by the connected IIDG_i, this line is identified as the fault section. For the passive branch, when the amplitudes of all harmonic currents measured by the IED at head of the protected line is much larger than those measured by the IED at remote-end, this branch can be also identified as the fault section. Otherwise, the fault is identified as an external fault, and the protection is restored.

In backup protection for an active branch(line), the line is deemed to be the faulted section if the imaginary part of the impedance from the connected IIDG_i nears zero, while simultaneously, there is a notable decrease in the imaginary parts from other IIDGs. For a passive line, an internal fault is suggested by a substantial reduction in the effective values of

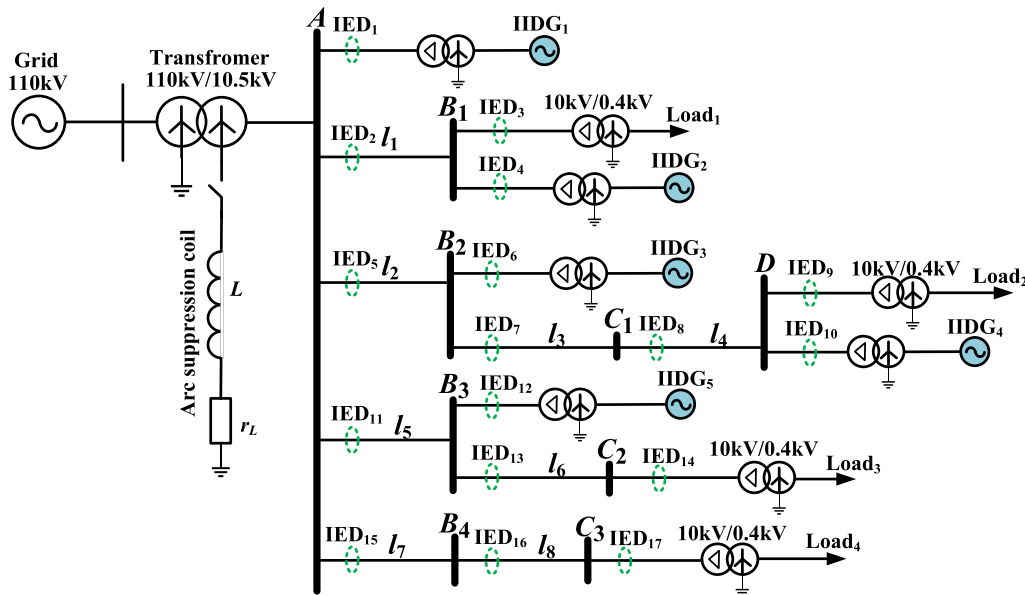


FIGURE 14. The tested active distribution network with high proportion IIDGs.

the imaginary parts of the impedance from all IIDGs on that line.

In particular, it is important to consider the possibility of IIDG disconnection faults. If an active branch(line) fails to detect the presence of corresponding harmonics, it indicates a potential disconnection fault with the IIDG. In such cases, the protection criterion for passive branches(lines) will be automatically activated to ensure the safety and reliability of the network.

IV. CASE STUDY

To validate the effectiveness of the proposed protection scheme, a 10.5kV active distribution network with a frequency of 50Hz is constructed in MATLAB/Simulink, as depicted in Figure 14. The network comprises a significant proportion of IIDGs, with a benchmark capacity of 100MVA and sampling frequency at 2.5kHz [27]. IIDG₁-IIDG₅ employ a droop control strategy, each with a rated capacity of 1MW. These IIDGs generate a harmonic voltage of one frequency with an amplitude of 0.1 p.u., which is superimposed on the fundamental modulation voltage produced by the conventional control loop.

When a nonlinear load is connected to a distribution network system with Integrated and Interconnected Distributed Generators (IIDG), the current flowing through the relay protection devices comprises not only the harmonic currents injected by the IIDG but also those introduced by the nonlinear load. Currently, typical nonlinear loads can be categorized into three types: ferromagnetic saturation, power electronic switching, and arc discharge. These loads primarily contribute to the generation of odd harmonics, including the 3rd, 5th, 7th, 9th, and 11th, as noted in [23] and [29]. To mitigate the impact of harmonics introduced by

TABLE 4. Fault scenarios.

Scenarios	S ₁	S ₂	S ₃	S ₄	S ₅	S ₆
Fault type	ABC	ABC	AB	AB	AB-G	AB-G
Fault location	<i>l</i> ₁	<i>l</i> ₃	<i>l</i> ₄	<i>l</i> ₆	<i>l</i> ₇	<i>l</i> ₈
Fault resistance(Ω)	0.1	0.1	20	20	100	100

nonlinear loads, IIDG is configured to inject even harmonic currents.

The harmonic frequencies for IIDG₁-IIDG₅ are 600Hz, 300Hz, 400Hz, 700Hz, and 500Hz, respectively. Loads 1 to 4 have a rated capacity of (0.6+j0.03) MVA. The length of all transmission lines is 2km, with the per unit values of positive sequence and zero sequence lines are (0.193+j0.107) Ω/km and (0.7+j1.221) Ω/km, respectively. The impedance of the grid-side line is set to 10 Ω.

A. INFLUENCE OF FAULT TYPE, LOCATION AND FAULT RESISTANCE

In this paper, six fault scenarios as shown in Table 4 are set up to test the performance of the proposed protection criteria under different fault types, locations, and fault resistance. These scenarios will also be continued in the following sections.

When a fault occurs, IIDGs inject harmonics, and the IED at the beginning of the line can analyze the harmonic current to obtain the amplitude information of each harmonic. Figure 15 shows the current and harmonic in *l*₂ under fault scenario S₁. Among them, Figure 15(a) represents the current waveform after injecting harmonics, clearly exhibiting distinct harmonic characteristics. Figure 15(b) presents the analysis results from IED₅, indicating the amplitude values

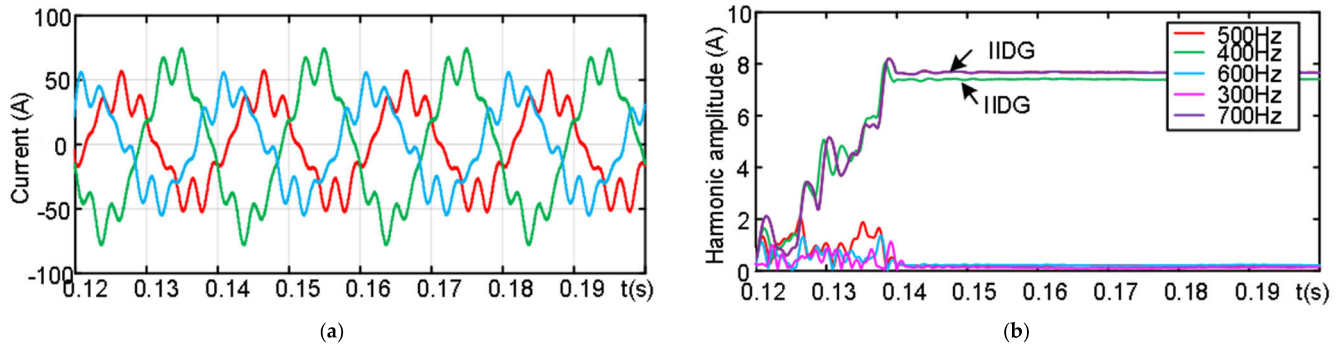


FIGURE 15. Current and harmonic in line l_2 under fault scenario S_1 . (a) Waveform of current; (b) Harmonic analysis results.

TABLE 5. Analysis of IED₇, IED₈, and IED₁₀ under different fault conditions and the corresponding protection results.

IED	Branch status	Scenarios	Harmonic with maximum amplitude	Harmonic with minimum amplitude	Mean amplitude of harmonics(p.u.)	Result
IED ₇	active	S ₁	700Hz	600Hz	/	External fault
		S ₂	400Hz	700Hz	/	Internal fault
		S ₃	700Hz	600Hz	/	External fault
		S ₄	700Hz	600Hz	/	External fault
		S ₅	700Hz	600Hz	/	External fault
		S ₆	700Hz	600Hz	/	External fault
IED ₈	active	S ₁	700Hz	600Hz	/	External fault
		S ₂	700Hz	600Hz	/	External fault
		S ₃	400Hz	700Hz	/	Internal fault
		S ₄	700Hz	600Hz	/	External fault
		S ₅	700Hz	600Hz	/	External fault
		S ₆	700Hz	600Hz	/	External fault
IED ₁₀	active	S ₁	700Hz	600Hz	/	External fault
		S ₂	700Hz	600Hz	/	External fault
		S ₃	700Hz	600Hz	/	External fault
		S ₄	700Hz	600Hz	/	External fault
		S ₅	700Hz	600Hz	/	External fault
		S ₆	700Hz	600Hz	/	External fault

for each harmonic in l_2 . Due to the connection of IIDG₃ and IIDG₄ at the end of this branch, the harmonic amplitudes of 400Hz and 700Hz are obviously larger than the other ones.

With different fault types, locations, and fault resistances, the protection results of the proposed protection scheme in active distribution networks with high proportion IIDGs are presented in Tables 5 and 6, respectively. IED₇, IED₈, and IED₁₀ are located in the active branch. As shown in Table 5, when a three-phase short circuit fault occurs in l_3 with a fault resistance (R_F) of 0.1 Ω , IED₇ indicates that the maximum amplitude harmonic frequency is 400Hz, and the minimum amplitude harmonic frequency is 700Hz. IED₈ at the end of the l_3 reveals that the maximum amplitude harmonic frequency is 700Hz, and the minimum amplitude harmonic frequency is 600Hz. Considering the system configuration, the harmonic of 700Hz is introduced by IIDG₄ of the active branch where IED₇ and IED₈ are located. Therefore, based on the provided data, the internal fault criteria for the active branch are satisfied, allowing for an accurate determination that the fault is located in l_3 . For the transmission line l_4 , IED₈ serves as the head-end device, while IED₁₀ operates as the remote-end one. The observed frequencies with the

maximum and minimum amplitudes at both IED₈ and IED₁₀ are consistent with the fault signature expected within the l_4 segment.

Similarly, the data and corresponding protection results of IED₁₆ and IED₁₇ on passive branch under different fault scenarios are listed in Table 6. When a two-phase grounding short circuit fault occurs in the l_8 with RF of 100 Ω , the mean amplitude of harmonics (p.u.) obtained by IED₁₆ is 2.102, which is much greater than the 0.011 given by IED₁₇ at the end of the branch. Satisfying the criteria for internal fault of passive branch can correctly determine that the accident is within the l_8 branch.

Based on the above analysis, it can be found that the protection scheme proposed in this paper is not affected by fault type, location, and fault resistance as it is based on the difference in features of harmonics at the beginning and end of the line.

B. INFLUENCE OF THE DISCONNECTION OF IIDGS

To analyze the influence of IIDG disconnection during a fault on the protection performance of the proposed method, IIDG₄ is disconnected, resulting in the branch where IIDG₄

TABLE 6. Analysis of IED₁₆ and IED₁₇ under different fault conditions and the corresponding protection results.

IED	Branch status	Scenarios	Harmonic with maximum amplitude	Harmonic with minimum amplitude	Mean amplitude of harmonics(p.u.)	Result
IED ₁₆	passive	S ₁	/	/	0.966	External fault
		S ₂	/	/	0.917	External fault
		S ₃	/	/	0.538	External fault
		S ₄	/	/	0.591	External fault
		S ₅	/	/	0.418	External fault
		S ₆	/	/	2.102	Internal fault
IED ₁₇	passive	S ₁	/	/	0.966	External fault
		S ₂	/	/	0.917	External fault
		S ₃	/	/	0.538	External fault
		S ₄	/	/	0.591	External fault
		S ₅	/	/	0.418	External fault
		S ₆	/	/	0.011	External fault

TABLE 7. Analysis of IED₇, IED₈, and IED₁₀ under different fault conditions after disconnection of IIDG₄ and the protection results.

IED	Branch status	Scenarios	Harmonic with maximum amplitude	Harmonic with minimum amplitude	Mean amplitude of harmonics(p.u.)	Result
IED ₇	passive	S ₁	/	/	1.112	External fault
		S ₂	/	/	3.297	Internal fault
		S ₃	/	/	0.571	External fault
		S ₄	/	/	0.565	External fault
		S ₅	/	/	0.397	External fault
		S ₆	/	/	0.299	External fault
IED ₈	passive	S ₁	/	/	1.112	External fault
		S ₂	/	/	0.007	External fault
		S ₃	/	/	2.916	Internal fault
		S ₄	/	/	0.565	External fault
		S ₅	/	/	0.397	External fault
		S ₆	/	/	0.299	External fault
IED ₁₀	active	S ₁	/	/	1.112	External fault
		S ₂	/	/	0.007	External fault
		S ₃	/	/	0.002	External fault
		S ₄	/	/	0.565	External fault
		S ₅	/	/	0.397	External fault
		S ₆	/	/	0.299	External fault

is originally located becoming a passive branch. Only the remaining four IIDGs inject harmonic current in this scenario. The protection results of the proposed protection scheme are shown in Table 7. After IIDG₄ is disconnected from the network, the relay protection devices of l_3 and l_4 activate the passive branch protection criterion. According to Table 7, under fault scenario S₂, IED₇ at the head-end of l_3 and IED₈ at the head-end of l_4 provide data that satisfies the internal fault criteria for passive branch, while data displayed by IED₈ and IED₁₀ also satisfies the internal fault criteria for passive branch when fault scenario S₃ occurs. These indicate the disconnection of IIDGs will not affect the accuracy of our proposed protection criteria. Therefore, the proposed protection scheme is robust and can accurately determine fault locations even when IIDGs are disconnected from the network during a fault.

C. INFLUENCE OF THE PERMEABILITY OF IIDGS

Consideration should also be given to the permeability of IIDGs when protecting active distribution networks with high proportion of IIDGs, along with the disconnection of IIDGs.

In this paper, the influence of adjusting the permeability of renewable energy sources is explored by modifying the impedance of the grid-side line. The proposed protection scheme is evaluated by adjusting the grid-side impedance to 30 Ω. The protection results are presented in Tables 8 and 9. It is evident that the proposed protection criterion effectively differentiates between internal and external faults. Moreover, the variations in the permeability of IIDGs have no influence on the effectiveness of the proposed protection scheme.

D. INFLUENCE OF NON-LINEAR LOAD CONNECTION

The widespread adoption of electronic devices, the incorporation of renewable energy sources, the growing demand for electric vehicle charging infrastructure, and the need for sophisticated energy management systems have collectively contributed to a significant shift in the load composition of active distribution networks. Nonlinear loads are increasingly becoming a prominent element within these networks. Consequently, it is imperative to examine the repercussions that the integration of nonlinear loads may have on the protection efficacy of the network. To this end, a simulation is conducted

TABLE 8. Analysis of Analysis of IED₇, IED₈, and IED₁₀ under different fault conditions after permeability of IIDGs and the protection results.

IED	Branch status	Scenarios	Harmonic with maximum amplitude	Harmonic with minimum amplitude	Mean amplitude of harmonics(p.u.)	Result
IED ₇	active	S ₁	700Hz	600Hz	/	External fault
		S ₂	400Hz	700Hz	/	Internal fault
		S ₃	700Hz	600Hz	/	External fault
		S ₄	700Hz	600Hz	/	External fault
		S ₅	700Hz	600Hz	/	External fault
		S ₆	700Hz	600Hz	/	External fault
IED ₈	active	S ₁	700Hz	600Hz	/	External fault
		S ₂	700Hz	600Hz	/	External fault
		S ₃	400Hz	700Hz	/	Internal fault
		S ₄	700Hz	600Hz	/	External fault
		S ₅	700Hz	600Hz	/	External fault
		S ₆	700Hz	600Hz	/	External fault
IED ₁₀	active	S ₁	700Hz	600Hz	/	External fault
		S ₂	700Hz	600Hz	/	External fault
		S ₃	700Hz	600Hz	/	External fault
		S ₄	700Hz	600Hz	/	External fault
		S ₅	700Hz	600Hz	/	External fault
		S ₆	700Hz	600Hz	/	External fault

TABLE 9. Analysis of IED₁₆ and IED₁₇ under different fault conditions after permeability of IIDGs and the corresponding protection results.

IED	Branch status	Scenarios	Harmonic with maximum amplitude	Harmonic with minimum amplitude	Mean amplitude of harmonics(p.u.)	Result
IED ₁₆	passive	S ₁	/	/	0.867	External fault
		S ₂	/	/	0.871	External fault
		S ₃	/	/	0.486	External fault
		S ₄	/	/	0.411	External fault
		S ₅	/	/	0.301	External fault
		S ₆	/	/	1.897	Internal fault
IED ₁₇	passive	S ₁	/	/	0.867	External fault
		S ₂	/	/	0.871	External fault
		S ₃	/	/	0.486	External fault
		S ₄	/	/	0.411	External fault
		S ₅	/	/	0.301	External fault
		S ₆	/	/	0.027	External fault

TABLE 10. Analysis of Analysis of IED₇, IED₈, and IED₁₀ under different fault conditions with a nonlinear load connection and the corresponding protection results.

IED	Branch status	Scenarios	Harmonic with maximum amplitude	Harmonic with minimum amplitude	Mean amplitude of harmonics(p.u.)	Result
IED ₇	active	S ₁	700Hz	600Hz	/	External fault
		S ₂	400Hz	700Hz	/	Internal fault
		S ₃	700Hz	600Hz	/	External fault
		S ₄	700Hz	600Hz	/	External fault
		S ₅	700Hz	600Hz	/	External fault
		S ₆	700Hz	600Hz	/	External fault
IED ₈	active	S ₁	700Hz	600Hz	/	External fault
		S ₂	700Hz	600Hz	/	External fault
		S ₃	400Hz	700Hz	/	Internal fault
		S ₄	700Hz	600Hz	/	External fault
		S ₅	700Hz	600Hz	/	External fault
		S ₆	700Hz	600Hz	/	External fault
IED ₁₀	active	S ₁	700Hz	600Hz	/	External fault
		S ₂	700Hz	600Hz	/	External fault
		S ₃	700Hz	600Hz	/	External fault
		S ₄	700Hz	600Hz	/	External fault
		S ₅	700Hz	600Hz	/	External fault
		S ₆	700Hz	600Hz	/	External fault

to validate the operational conditions: a diode uncontrolled rectifier, equipped with DC side capacitance, resistance, and inductance parameters denoted as $C_{dc} = 0.1\text{mF}$, $R_{dc} = 5\Omega$

and $L_{dc} = 5\text{mH}$, respectively, is connected to bus D through an interface transformer. The protection results of the proposed scheme are presented in Tables 10 and 11. Through

TABLE 11. Analysis of IED₁₆ and IED₁₇ under different fault conditions with a nonlinear load connection and the protection results.

IED	Branch status	Scenarios	Harmonic with maximum amplitude	Harmonic with minimum amplitude	Mean amplitude of harmonics(p.u.)	Result
IED ₁₆	passive	S ₁	/	/	0.753	External fault
		S ₂	/	/	0.767	External fault
		S ₃	/	/	0.531	External fault
		S ₄	/	/	0.520	External fault
		S ₅	/	/	0.489	External fault
		S ₆	/	/	1.797	Internal fault
IED ₁₇	passive	S ₁	/	/	0.753	External fault
		S ₂	/	/	0.767	External fault
		S ₃	/	/	0.531	External fault
		S ₄	/	/	0.520	External fault
		S ₅	/	/	0.489	External fault
		S ₆	/	/	0.017	External fault

TABLE 12. Analysis of IED₇ and IED₈ under different fault conditions during the activation of backup protection and the protection results.

IED	Branch status	$\left \text{Im} \left(Z_{Linc}^h \right) \right $ in the absence of any fault (600Hz, 300Hz, 400Hz, 700Hz, 500Hz)(p.u.)	Scenarios	$\left \text{Im} \left(Z_{Linc}^h \right) \right $ obtained during a fault occurrence (600Hz, 300Hz, 400Hz, 700Hz, 500Hz)(p.u.)	Result
IED ₇	active	(31.872, 15.936, 21.248, 37.184, 26.560)	S ₁	(31.872, 0.002, 21.248, 37.184, 26.560)	External fault
			S ₂	(14.3424, 7.1712, 9.5616, 0.005, 11.952)	Internal fault
			S ₃	(31.872, 15.936, 21.248, 0.002, 26.560)	External fault
			S ₄	(31.872, 15.936, 21.248, 37.184, 26.560)	External fault
			S ₅	(31.872, 15.936, 21.248, 37.184, 26.560)	External fault
			S ₆	(31.872, 15.936, 21.248, 37.184, 26.560)	External fault
IED ₈	active	(31.872, 15.936, 21.248, 37.184, 26.56)	S ₁	(31.872, 0.001, 21.248, 37.184, 26.560)	External fault
			S ₂	(0.009, 0.002, 0.010, 37.184, 0.008)	External fault
			S ₃	(17.5296, 8.7648, 11.6864, 0.001, 14.608)	Internal fault
			S ₄	(31.872, 15.936, 21.248, 37.184, 26.560)	External fault
			S ₅	(31.872, 15.936, 21.248, 37.184, 26.560)	External fault
			S ₆	(31.872, 15.936, 21.248, 37.184, 26.560)	External fault

TABLE 13. Analysis of IED₁₆ and IED₁₇ under different fault conditions during the activation of backup protection and the protection results.

IED	Branch status	$\left \text{Im} \left(Z_{Linc}^h \right) \right $ in the absence of any fault (600Hz, 300Hz, 400Hz, 700Hz, 500Hz)(p.u.)	Scenarios	$\left \text{Im} \left(Z_{Linc}^h \right) \right $ obtained during a fault occurrence (600Hz, 300Hz, 400Hz, 700Hz, 500Hz)(p.u.)	Result
IED ₁₆	passive	(31.872, 15.936, 21.248, 37.184, 26.560)	S ₁	(31.872, 15.936, 21.248, 37.184, 26.560)	External fault
			S ₂	(31.872, 15.936, 21.248, 37.184, 26.560)	External fault
			S ₃	(31.872, 15.936, 21.248, 37.184, 26.560)	External fault
			S ₄	(31.872, 15.936, 21.248, 37.184, 26.560)	External fault
			S ₅	(0.001, 0.000, 0.002, 0.002, 0.001)	External fault
			S ₆	(14.3424, 7.1712, 9.5616, 16.7328, 11.952)	Internal fault
IED ₁₇	passive	(28.615, 14.308, 19.077, 33.384, 23.846)	S ₁	(28.615, 14.308, 19.077, 33.384, 23.846)	External fault
			S ₂	(28.615, 14.308, 19.077, 33.384, 23.846)	External fault
			S ₃	(28.615, 14.308, 19.077, 33.384, 23.846)	External fault
			S ₄	(28.615, 14.308, 19.077, 33.384, 23.846)	External fault
			S ₅	(0.003, 0.001, 0.000, 0.001, 0.001)	External fault
			S ₆	(0.001, 0.001, 0.000, 0.001, 0.001)	External fault

the analysis of simulation data, it is evident that the characteristics of faults, whether occurring inside or outside the designated area, still conform to the criteria established by the proposed method. This confirmation demonstrates that the proposed method retains its capability to correctly

identify the locations of faults even when nonlinear loads are connected to the system. These results highlight the reliability and effectiveness of the proposed fault location approach in active distribution networks that are characterized by a substantial integration of nonlinear loads.

E. INFLUENCE OF COMMUNICATION FAILURE BETWEEN ADJACENT IEDS

In active distribution networks, communication failures among adjacent IEDs can arise due to physical connection issues, electromagnetic interference, configuration mistakes, network bottlenecks, or equipment malfunctions. When such disruptions occur, main protection becomes inoperative, prompting the activation of backup protection measures. The performance of backup protection under these adverse conditions is assessed, with Tables 12 and 13 illustrating the data analysis for IEDs 7, 8, 16, and 17 in the absence of faults. Specifically, IED7, which is on an active branch, exhibits the lowest impedance reading at 700Hz, and the current induced by the corresponding IIDG is decreased, satisfying the backup protection criteria for active branch faults. This finding is consistent with fault scenario S_2 , validating the reliability of the backup protection for active branches. For IED₁₆ on the passive branch, the impedance change generated by S_6 on the l_8 confirms the correctness of the backup protection criteria for the passive branch. It is worth noting that the IED₁₇ located down-stream of l_8 also fully meets the external fault characteristics of the passive branch area, proving capability of the backup protection to distinctly differentiate between faults occurring upstream and downstream. In conclusion, the data provided verifies the effectiveness of the backup protection outlined in this paper for active distribution networks.

V. CONCLUSION

An injected harmonic feature based protection scheme for active distribution network with high proportion IIDGs is addressed in this paper, taking into account the flexible controllability of IIDGs. This scheme consists of a main protection mechanism utilizing current features and a backup protection mechanism utilizing impedance features. The main conclusions are as follows:

- 1) The required harmonics with different orders are generated and injected by controlling IIDGs during a fault. When the main protection is operational, for active branches, the connected IIDG injects the minimum amplitude of the corresponding harmonic at the fault line, while its maximum amplitude can be found at the non-fault line. For passive branches, the harmonic current amplitudes at the head-end are much larger than those at the remote-end. Backup protection is activated to supplement the system when the main protection fails. For active branches experiencing internal faults, two main indicators are observed: a significant impedance change at the resonant frequency of the line from the injected harmonics and the impedance caused by the connected IIDG on this line approaches zero.
- 2) The proposed criterion of main protection is constructed using all harmonic current frequencies and amplitudes injected by different IIDGs to represent the fault direction. Only the head-end currents of the line

connected to bus are measured and collected by IED installed at that line. The main protection only needs to interface with the adjacent level. This streamlined communication protocol results in a reduced data transfer volume and minimal bandwidth requirements. Consequently, this approach enhances protection efficiency and reduces communication costs, offering a more optimized and cost-effective solution for fault management in active distribution networks

- 3) The distinct harmonic current profiles associated with various fault types enable this method to inherently select the faulted phase, leveraging the unique harmonic signatures for accurate fault identification. Thus, it is effective for different fault types, fault locations, and fault resistances. When the main protection fails, the backup protection can also achieve fault localization. It is not affected by the disconnection of any IIDG or changes in the proportion of IIDGs connected to the distribution networks, as well as the connection of nonlinear loads.

For the proposed scheme, in case where the scale of the active distribution network is extensive, there may be restrictions on the number of available frequencies for injected harmonics, leading to the scenarios where different active branches(lines) inject harmonics at the same frequency. Under such circumstances, the proposed scheme may fail to detect and localize faults effectively. Future research will be dedicated to addressing this issue more comprehensively.

REFERENCES

- [1] A. Barranco-Carlos, C. Orozco-Henao, J. Marín-Quintero, J. Mora-Flórez, and A. Herrera-Orozco, "Adaptive protection for active distribution networks: An approach based on fuses and relays with multiple setting groups," *IEEE Access*, vol. 11, pp. 31075–31091, 2023, doi: [10.1109/ACCESS.2023.3261827](https://doi.org/10.1109/ACCESS.2023.3261827).
- [2] W. Jin, S. Zhang, J. Li, M. Feng, S. Feng, and Y. Lu, "A novel differential protection scheme for distribution lines under weak synchronization conditions considering DG characteristics," *IEEE Access*, vol. 11, pp. 86561–86574, 2023.
- [3] J.-S. Kim, E.-C. Lee, and S.-Y. Yun, "Protection system for LVDC distribution networks using a fault current-limiting converter and protection zones," *IEEE Access*, vol. 11, pp. 75555–75572, 2023.
- [4] F. Coffele, C. Booth, and A. Dysko, "An adaptive overcurrent protection scheme for distribution networks," *IEEE Trans. Power Del.*, vol. 30, no. 2, pp. 561–568, Apr. 2015.
- [5] H. Muda and P. Jena, "Superimposed adaptive sequence current based microgrid protection: A new technique," *IEEE Trans. Power Del.*, vol. 32, no. 2, pp. 757–767, Apr. 2017.
- [6] H. H. Zeineldin, H. M. Sharaf, D. K. Ibrahim, and E. E.-D.-A. El-Zahab, "Optimal protection coordination for meshed distribution systems with DG using dual setting directional over-current relays," *IEEE Trans. Smart Grid*, vol. 6, no. 1, pp. 115–123, Jan. 2015.
- [7] M. Ghotbi-Maleki, R. M. Chabanloo, H. H. Zeineldin, and S. M. H. Miangafsheh, "Design of setting group-based overcurrent protection scheme for active distribution networks using MILP," *IEEE Trans. Smart Grid*, vol. 12, no. 2, pp. 1185–1193, Mar. 2021.
- [8] A. Sinclair, D. Finney, D. Martin, and P. Sharma, "Distance protection in distribution systems: How it assists with integrating distributed resources," *IEEE Trans. Ind. Appl.*, vol. 50, no. 3, pp. 2186–2196, May/Jun. 2014.
- [9] B. Mahamedi and J. E. Fletcher, "The equivalent models of grid-forming inverters in the sequence domain for the steady-state analysis of power systems," *IEEE Trans. Power Syst.*, vol. 35, no. 4, pp. 2876–2887, Jul. 2020.

- [10] K. Jia, T. Bi, Z. Ren, D. W. P. Thomas, and M. Sumner, "High frequency impedance based fault location in distribution system with DGs," *IEEE Trans. Smart Grid*, vol. 9, no. 2, pp. 807–816, Mar. 2018.
- [11] Z. Yang, K. Jia, Y. Fang, Z. Zhu, B. Yang, and T. Bi, "High-frequency fault component-based distance protection for large renewable power plants," *IEEE Trans. Power Electron.*, vol. 35, no. 10, pp. 10352–10362, Oct. 2020.
- [12] H. Gao, J. Li, and B. Xu, "Principle and implementation of current differential protection in distribution networks with high penetration of DGs," *IEEE Trans. Power Del.*, vol. 32, no. 1, pp. 565–574, Feb. 2017.
- [13] B. Han, H. Li, G. Wang, D. Zeng, and Y. Liang, "A virtual multi-terminal current differential protection scheme for distribution networks with inverter-interfaced distributed generators," *IEEE Trans. Smart Grid*, vol. 9, no. 5, pp. 5418–5431, Sep. 2018.
- [14] C. Zhou, G. Zou, L. Zang, and X. Du, "Current differential protection for active distribution networks based on improved fault data self-synchronization method," *IEEE Trans. Smart Grid*, vol. 13, no. 1, pp. 166–178, Jan. 2022.
- [15] C. Zhou, G. Zou, S. Zhang, M. Zheng, J. Tian, and T. Du, "Mathematical morphology based fault data self synchronization method for differential protection in distribution networks," *IEEE Trans. Smart Grid*, vol. 14, no. 4, pp. 2607–2620, Jul. 2023.
- [16] X. Li and Y. Lu, "Improved amplitude differential protection scheme based on the frequency spectrum index for distribution networks with DFIG-based wind DGs," *IEEE Access*, vol. 8, pp. 64225–64237, 2020, doi: 10.1109/ACCESS.2020.2984031.
- [17] G. Chen, Y. Liu, and Q. Yang, "Impedance differential protection for active distribution network," *IEEE Trans. Power Del.*, vol. 35, no. 1, pp. 25–36, Feb. 2020.
- [18] X. Zheng, C. Chao, Y. Weng, H. Ye, Z. Liu, P. Gao, and N. Tai, "High-frequency fault analysis-based pilot protection scheme for a distribution network with high photovoltaic penetration," *IEEE Trans. Smart Grid*, vol. 14, no. 1, pp. 302–314, Jan. 2023.
- [19] C. García-Ceballos, S. Pérez-Londoño, and J. Mora-Flórez, "Compensated fault impedance estimation for distance-based protection in active distribution networks," *Int. J. Electr. Power Energy Syst.*, vol. 151, Sep. 2023, Art. no. 109114.
- [20] F. Özveren and Ö. Usta, "A power based integrated protection scheme for active distribution networks against asymmetrical faults," *Electric Power Syst. Res.*, vol. 218, May 2023, Art. no. 109223.
- [21] J. Orozco-Álvarez, A. Herrera-Orozco, and J. Mora-Flórez, "Communication-less adaptive directional overcurrent protection strategy considering islanded mode detection in active distribution networks," *Results Eng.*, vol. 20, Dec. 2023, Art. no. 101538.
- [22] K. O. Oureilidis and C. S. Demoulias, "A fault clearing method in converter-dominated microgrids with conventional protection means," *IEEE Trans. Power Electron.*, vol. 31, no. 6, pp. 4628–4640, Jun. 2016.
- [23] Z. Chen, X. Pei, M. Yang, L. Peng, and P. Shi, "A novel protection scheme for inverter-interfaced microgrid (IIM) operated in islanded mode," *IEEE Trans. Power Electron.*, vol. 33, no. 9, pp. 7684–7697, Sep. 2018.
- [24] W. T. El-Sayed, M. A. Azzouz, H. H. Zeineldin, and E. F. El-Saadany, "A harmonic time-current-voltage directional relay for optimal protection coordination of inverter-based islanded microgrids," *IEEE Trans. Smart Grid*, vol. 12, no. 3, pp. 1904–1917, May 2021.
- [25] K. A. Saleh and A. Mehrizi-Sani, "Harmonic directional overcurrent relay for islanded microgrids with inverter-based DGs," *IEEE Syst. J.*, vol. 15, no. 2, pp. 2720–2731, Jun. 2021.
- [26] H. M. Ibrahim, M. S. El Moursi, and P.-H. Huang, "Adaptive roles of islanded microgrid components for voltage and frequency transient responses enhancement," *IEEE Trans. Ind. Informat.*, vol. 11, no. 6, pp. 1298–1312, Dec. 2015.
- [27] F. Blaabjerg, R. Teodorescu, M. Liserre, and A. V. Timbus, "Overview of control and grid synchronization for distributed power generation systems," *IEEE Trans. Ind. Electron.*, vol. 53, no. 5, pp. 1398–1409, Oct. 2006.
- [28] L. He, Z. Shuai, X. Zhang, X. Liu, Z. Li, and Z. J. Shen, "Transient characteristics of synchronverters subjected to asymmetric faults," *IEEE Trans. Power Del.*, vol. 34, no. 3, pp. 1171–1183, Jun. 2019.
- [29] K. C. Umeh, A. Mohamed, R. Mohamed, and A. Hussain, "Characterizing nonlinear load harmonics using fractal analysis," in *Proc. IEEE Int. Symp. Circuits Syst.*, vol. 5, May 2004, pp. 932–935.



HAIYING YU received the B.S. degree in accounting and the M.S. degree in the subject of Marxism and ideological political education from Changchun University of Science and Technology, Harbin, China, in 2003 and 2008, respectively, and the Ph.D. degree in business administration from the School of Management, Harbin Institute of Technology, Harbin, in 2013.

He is currently with Harbin Energy Innovation Digital Technology Company Ltd. His research interests include intelligent generating plant and digital twin.



ZHONGFENG LU received the B.S. and M.S. degrees in electrical engineering from Harbin Institute of Technology, Harbin, China, in 1999 and 2003, respectively, and the Ph.D. degree in electrical engineering from the School of Electrical Engineering and Automation, Harbin Institute of Technology, in 2009.

He is currently with Harbin Energy Innovation Digital Technology Company Ltd. His research interests include digital factory and digital government.



YULIANG LIU received the B.S. degree in aircraft manufacture engineering and the M.S. degree in aerospace manufacturing engineering from Harbin Institute of Technology, Harbin, China, in 2008 and 2010, respectively, and the Ph.D. degree in mechatronic engineering from the School of Mechanical and Electrical Engineering, Harbin Institute of Technology, in 2016.

He is currently with Harbin Energy Innovation Digital Technology Company Ltd. His research interests include intelligent generating plant, digital factory, and digital twin.



YANG GAO received the B.S. degree in business and management studies from the University of Bradford, Bradford, U.K., in 2006, the M.S. degree in management from the University of Nottingham, Nottingham, U.K., in 2007, and the Ph.D. degree in business administration from the School of Management, Harbin Institute of Technology University, Harbin, China, in 2011.

She is currently with Harbin Normal University. Her research interests include e-commerce and digital innovation.



JINGYING WAN received the B.S. degree in network engineering from Shijiazhuang Tiedao University, China, in 2016, and the M.S. degree in electrical engineering from the Central South University, China, in 2020. She is currently pursuing the Ph.D. degree with the College of Electrical and Information Engineering, Hunan University, Changsha, China.

Her research interests include fast fault diagnosis and the isolation of AC/DC hybrid networks.

...